

RESEARCH

Open Access



Numerical simulation study on the evolution characteristics of the stress induced by mining in deep adjacent working faces

Shoulong Ma¹, Mingwei Zhang^{2*}, Lu Ma¹, Zhuangcai Tian², Xue Li¹ and Zhenhao Su¹

Abstract

Background The mining-induced stress in the surrounding rock after coal seam mining is the primary cause of damage and failure of the surrounding rock in the mining area. However, the magnitude and direction of the stress field induced by mining in the overburden strata during the excavation process of deep and adjacent coal seams are not yet clear, and it is difficult to determine how adjacent working faces interact with each other.

Results In this study, a large-scale numerical model was built using FLAC3D (Fast Lagrange Analysis Continua) to simulate the sequential mining process of three adjacent working faces (No.1, No.2, and No.3) in Liuzhuang Coal Mine located in southern China. The results showed that the maximum height of plastic zone development after mining in the No.1 working face was 41 m, and the maximum height of plastic zone development was 33.8 m away from the 13 coal seam. It did not affect the top and bottom of the No.3 working face. The development height of the plastic zone on the roof of the No.2 working face after mining was 52m, and the top and bottom plates of the No.3 working face remained intact. The plastic zone of the floor of the No.3 working face after mining was not communicated with the plastic zone of the roof of the No.1 and No.2 working faces. There was a complete rock layer between the two coal seams, and there was not the mutual influence of the mining activities. During the mining process of working faces No.1 and No.2, the range of dynamic pressure influence was extended up to 100m ahead of the working face. During the mining process of the No.3 working face, the range of dynamic pressure influence was 120 m ahead of the working face. The No.1 working face goaf and the mining of No.2 working face had not disturbance to the No.3 working face.

Conclusions After the mining of No.1 and No.2 working faces, the stress in the goaf significantly decreased, and the lateral support stress concentration area of No.1 and No.2 working faces had a relatively small impact on the 13 coal seam. Therefore, the No.1 goaf and mining of No.2 working faces had not disturbance to No.3 working face.

Keywords Surrounding rock, Mining stress, Adjacent working faces, Dynamic pressure, Plastic zone

Introduction

The excavation of coal seams induces mining stress in the surrounding rock, which is the primary cause of damage and failure of the rock mass in the mining area. The spatiotemporal evolution and fracture process of the three-dimensional mining stress in the overburden strata of the working face are crucial for ensuring stable control of the surrounding rock in the mining area (Pirulli et al. 2017; Ti et al. 2021; Li et al. 2022). In the process, rock bursts

*Correspondence:

Mingwei Zhang
mingweizhang@cumt.edu.cn

¹ China Coal Xinji Energy Co., Ltd., Huainan 232001, People's Republic of China

² State Key Laboratory for Geomechanics and Deep Underground Engineering, China University of Mining and Technology, Xuzhou 221116, People's Republic of China



© The Author(s) 2023. **Open Access** This article is licensed under a Creative Commons Attribution 4.0 International License, which permits use, sharing, adaptation, distribution and reproduction in any medium or format, as long as you give appropriate credit to the original author(s) and the source, provide a link to the Creative Commons licence, and indicate if changes were made. The images or other third party material in this article are included in the article's Creative Commons licence, unless indicated otherwise in a credit line to the material. If material is not included in the article's Creative Commons licence and your intended use is not permitted by statutory regulation or exceeds the permitted use, you will need to obtain permission directly from the copyright holder. To view a copy of this licence, visit <http://creativecommons.org/licenses/by/4.0/>.

maybe occur and release large amounts of elastic strain energy accumulated in hard coal and rock mass (Zhang et al. 2018a, b; Qian et al. 2018). The stress field distribution in the surrounding rock is a fundamental basis for addressing technical challenges, such as mining plan design, coal and gas outburst prevention and control, and prediction and prevention of rock burst phenomena (Tang et al. 2021; Wo et al. 2022).

Extensive research has been conducted by many scholars on the evolution mechanism of stress fields and control challenges in deep mining surrounding rocks. Liu et al. (2015) proposed the existence of dynamic and static support pressures in longwall stopes and identified the formation and evolution of dynamic support pressure as a result of rock movement in the fractured zone of the stope roof. Lin et al. (2015) studied the stress evolution law of tunnel surrounding rock under different stress conditions and the alternating tensile and compressive states of surrounding rock through physical experiments. Zhou et al. (2016) utilized the stress relief method for mining stress monitoring and conducted an in-depth analysis of the evolution law of mining stress and the spatial relationship between the maximum principal stress and the peak support pressure. Through extensive research on the distribution characteristics of stress shells in the surrounding rock of the mining area, numerous studies have analyzed the main controlling factors for the expansion of cracks in the surrounding rock. The fracture zone of the surrounding rock mainly occurred in the low stress area of the stress shell (Wang et al. 2015; Xie et al. 2018a). Existing studies have analyzed the effects of mining height, mining depth, and face length on the surrounding rock mining stress field, revealing the mechanical mechanism of roof rock fracture by studying the mining stress, crack distribution, and overburden rock fracture patterns in deep mining areas (Li et al. 2018; Guo et al. 2018). Pang et al. (2023) proposed a three-dimensional mining stress disturbance coefficient calculation method based on the relationship between stress state and strength change through numerical simulation. The evolution characteristics of coal support pressure and plastic zone in the working face were studied through numerical simulation, and the main controlling factors of tunnel stress distribution were analyzed (Meng et al. 2016; Huang et al. 2019). A significant amount of research and analysis have been conducted on the spatiotemporal evolution laws of the three-dimensional stress of the bottom plate and the stress of the support bearing structure. It has been pointed out that the spatiotemporal correspondence of the deformation area of the surrounding rock in deep mine tunnels was the main reason for the segmented and repeated failure of tunnels (Zhou et al. 2016; Xie et al. 2018a; Zhang et al. 2018a, b; Peng et al. 2016). Physical

experiments and numerical simulations were commonly used to study the evolution law of stress in the surrounding rock of tunnels. Conventional methods were generally used to monitor the variation law of mining-induced stress on-site, but there was little research on the movement of overburden rock and main stress in the roof during the mining process of adjacent working faces (Zhang et al. 2018a, b; 2021; Wu et al. 2021; Luo et al. 2023). The research on the stress evolution law of surrounding rock under mining conditions in deep working faces was not comprehensive and in-depth enough.

The fracture of overburden strata in deep mining areas was caused by the mining stress state and the mutual transformation between different stress states. This directly affected the stability and failure process of the overlying strata. However, the magnitude and direction of the stress field induced by mining in the overburden strata during the excavation process of deep adjacent coal seams were not yet clear, and it was difficult to determine how adjacent working faces interact with each other. In this study, we used FLAC^{3D} (Fast Lagrange Analysis Continua) to construct a large-scale numerical model to simulate the sequential mining process of three adjacent working faces in Liuzhuang Coal Mine located in southern China. We analyzed the evolution law of mining stress and the impact of dynamic pressure, identified the roof plastic zone and roof subsidence characteristics in the mining process of each working face, and revealed the evolution law of mining dynamic stress and the influence range of dynamic pressure.

Methods

Based on the distribution characteristics and rock stratum parameters of three working faces in Liuzhuang Coal Mine (as shown in Table 1), a large-scale numerical calculation model was constructed using FLAC^{3D}. The model dimensions were 1000 m (Y) × 800 m (X) × 162 m (Z), consisting of a total of 624,000 units and 650,440 nodes (as depicted in Fig. 1). To eliminate the boundary effects during the numerical calculation process, the distance between the working face and the model boundary was set to be no less than 80 m. We simulated 13 coal seam (No.3 working face) was buried at a depth of 580 m, while another coal seam (No.1 and 2 working face) was buried at a greater depth of 654.8 m. The vertical distance between two coal seam was 74.8 m. Two coal seams have same properties. Properties and thickness of the rock layers were assumed according to bare log of Liuzhuang Coal Mine. The unit weight of the rock layer above the model was assumed to be 25kN/m³, and the equivalent load of the rock layer was calculated to be 10.8 MPa, which was applied to the upper boundary of the model. The strain softening model was used to calculate the

Table 1 Rock mechanics parameters of rock stratum

Number	Lithology	Density (kg/m ³)	Bulk modulus (Pa)	Shear modulus (Pa)	Cohesion (MPa)	Internal friction angle (°)	Tensile strength (MPa)
1	Mudstone	2652	2.54E+09	1.38E+09	1.30	30	0.43
2	Carbonaceous shale	2572	4.10E+09	2.58E+09	1.87	32	1.1
3	Siltstone	2596	1.09E+10	8.58E+09	17.24	43	2.29
4	Sandy mudstone	2686	4.11E+09	3.08E+09	7.06	35	1.00
5	13 Coal seam	1400	1.90E+09	9.30E+08	0.84	27	0.28
6	Fine sandstone	2730	8.18E+09	7.28E+09	18.13	45	2.29
7	Medium sandstone	2607	7.34E+09	6.62E+09	13.02	42	3.68

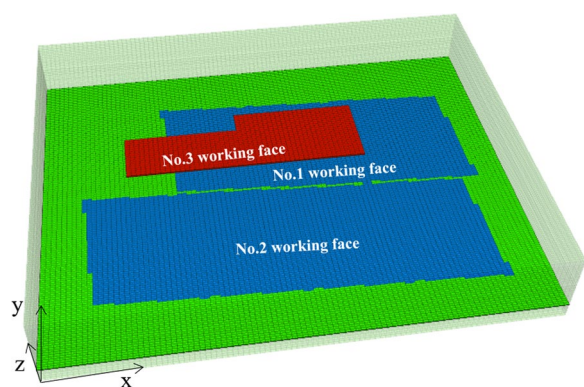


Fig. 1 Working face layout

constitutive model, and the fix command was applied to the surrounding and bottom surfaces of the model for boundary fixation. The initial crustal stress setting was based on the on-site crustal stress test results, and the lateral pressure coefficient of the model in the X direction was 0.6, while the lateral pressure coefficient of the model in the Y direction (i.e., the direction of the working face) was 0.8 (as shown in Fig. 1).

Utilizing the mining sequence of the working face in Liuzhuang Coal Mine, we conducted a simulation of

the mining process for the No.1, No.2, and No.3 working faces. We first simulated the mining of the No.1 working face, then simulated the mining of the No.2 working face, and finally simulated the mining of the No.3 working face. The vertical distance between the No.3 and No.2 working faces was found to be 74.8 m. The simulated advance length for the No.1 working face was 640 m, while the No.2 and No.3 working faces had simulated advance lengths of 800 m and 500 m, respectively (Fig. 1).

Results

Evolution law of plastic zone in roof

To investigate the distribution characteristics of the plastic zone after mining in the working face, a slice perpendicular to the x-axis was taken at the center of the model. The plastic zone distribution after mining in the No.1, No.2, and No.3 working faces was studied. Figure 2 illustrated the distribution of the plastic zone after mining in the No.1 working face. The results indicated that the plastic zone on the roof after mining in the No.1 working face exhibited a saddle-shaped distribution. The plastic zone above the two grooves has the highest development height, reaching a maximum height of 41 m. The maximum development height of the plastic zone was 33.8 m away from 13 coal seam. Therefore, the mining of the

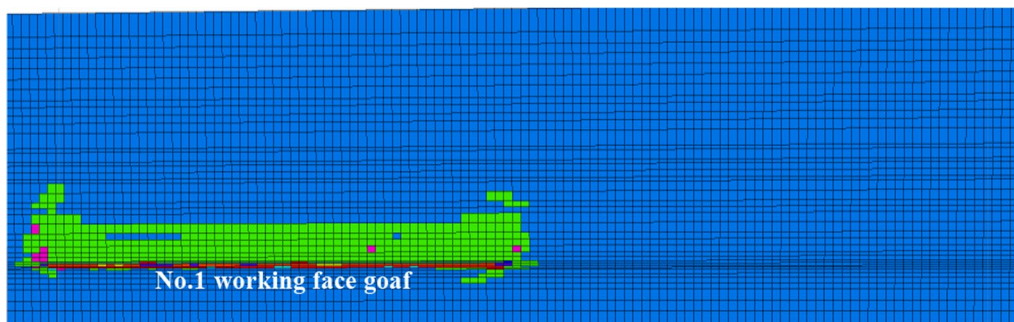


Fig. 2 Distribution of the plastic zone after mining in No.1 working face

No.1 working face has not affected the top and bottom of the No.3 working face.

The distribution of plastic zone after mining in No.2 working face was showed in Fig. 3. The height of plastic zone development on the roof of the No.2 working face after mining was 52 m, which was marginally higher than that of the No.1 working face (Fig. 3). The maximum height of plastic zone development was 22.8 m away from 13 coal seam, indicating that the top and bottom plates of the No.3 working face remained intact without any damage during the mining process of the No.1 working face.

The distribution of plastic zone after mining in No.3 working face was showed in Fig. 4. The development range of the plastic zone on the floor of the No.3 working face was relatively small (Fig. 4). The plastic zone on the floor of the No.3 working face was not connected with the plastic zones on the roof of the No.1 and No.2 working faces, and there was a complete rock layer between the two coal seams. This indicated that the mutual influence of mining activities on the two coal seam was relatively small.

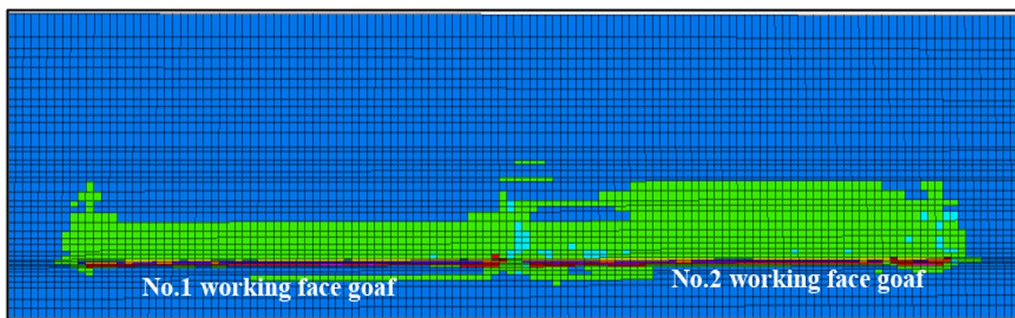


Fig. 3 Distribution of plastic zone after mining in No.2 working face

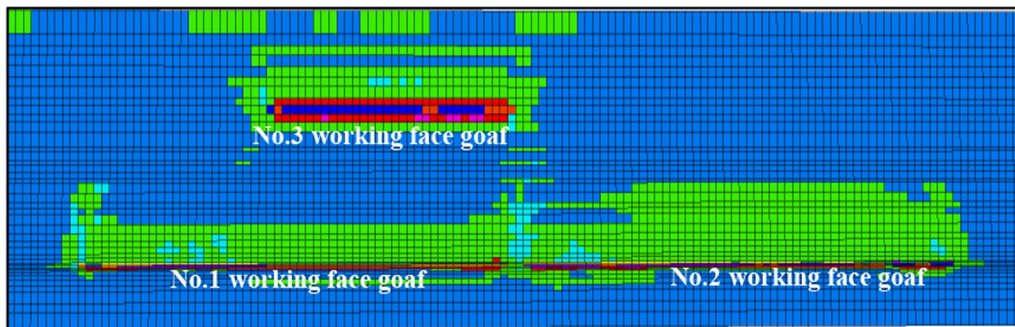


Fig. 4 Distribution map of the plastic zone after mining in the No.3 working face

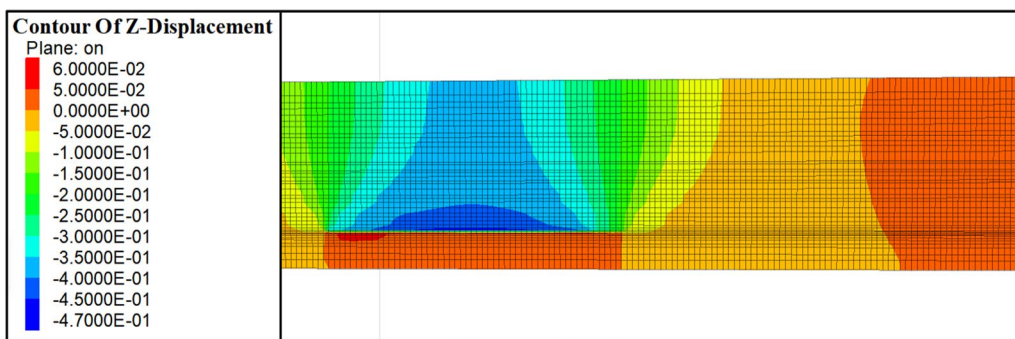


Fig. 5 Roof subsidence after mining in the No.1 working face

Roof subsidence law

Following the mining of the working face, a displacement cloud map was generated by slicing the model along the direction perpendicular to the x-axis at the midpoint. The objective was to investigate the subsidence law of the roof in the No.1, No.2, and No.3 working faces after sequential mining. Figure 5 illustrated the cloud map of the roof subsidence after mining in the No.1 working face. The results indicated that the maximum subsidence of the roof in the No.1 working face was 0.47 m, and the position of maximum subsidence was observed in the middle roof area of the working face (Fig. 5).

The cloud map of the roof subsidence after mining in the No.2 working face was showed in Fig. 6. The maximum roof subsidence after mining in the No.2 working face was 0.65 m, which was greater than the roof subsidence after mining in the No.1 working face (as shown in Fig. 6). The maximum subsidence was situated in the middle roof area of the No.2 working face. The No.3 working face was positioned above the No.1 and No.2 working faces. The coal and rock strata in proximity to the No.3 working face have undergone a certain degree of subsidence due to the influence of mining on both working faces, with a maximum subsidence of 0.42 m.

Considering the plastic distribution characteristics after mining on the No.1 and No.2 working faces (as illustrated in Figs. 2, 3), the maximum development height of the plastic zone after mining on the No.1 and No.2 working faces was still 28 m away from the 13 coal seam. Therefore, the impact of mining in the No.1 and No.2 working faces on the coal and rock layers in the No.3 working face area was relatively small.

Figure 7 displayed the cloud map of roof subsidence after mining in the No.3 working face. The maximum roof subsidence after mining in the No.3 working face was 1.3 m (as shown in Fig. 7). The subsidence was more than twice as much as the subsidence of No.1 and No.2 working face. Due to the large mining height of the No.3 working face, the roof subsidence was relatively significant, and the maximum subsidence position was located in the middle roof area of the working face.

Discussion

Evolution law of mining stress and influence range of dynamic pressure in No.1 working face

The vertical stress of the coal seam in the No.1 working face was sliced to analyze the evolution law of support stress during the mining process. Figure 8 showed the distribution of support stress in the No.1 working face.

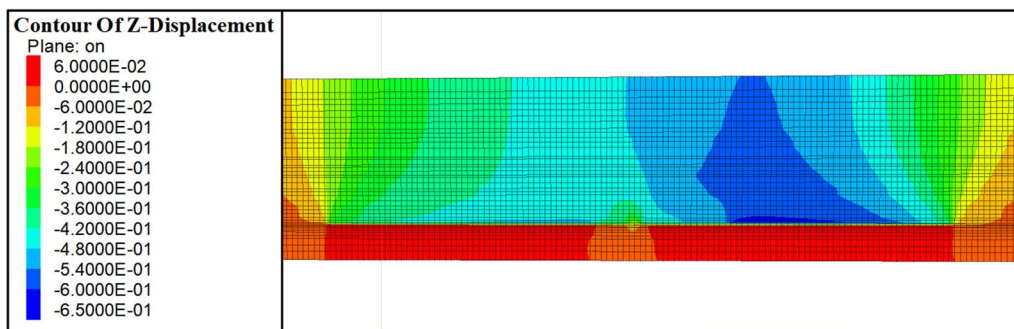


Fig. 6 Roof subsidence after mining in the No.2 working face

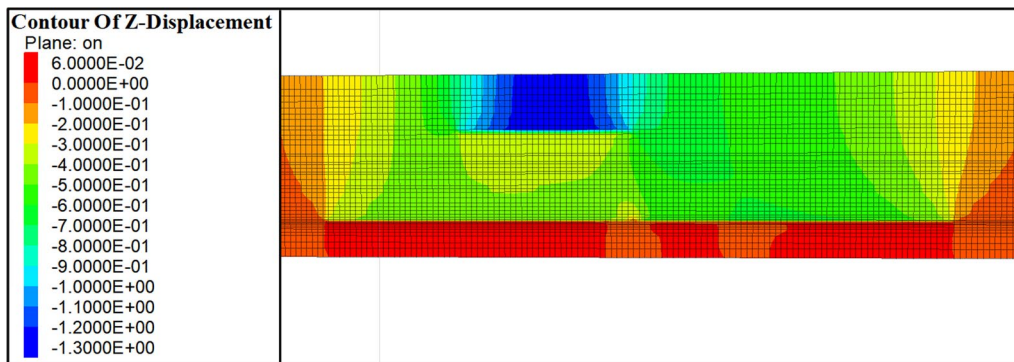


Fig. 7 Roof subsidence after mining in the No.3 working face

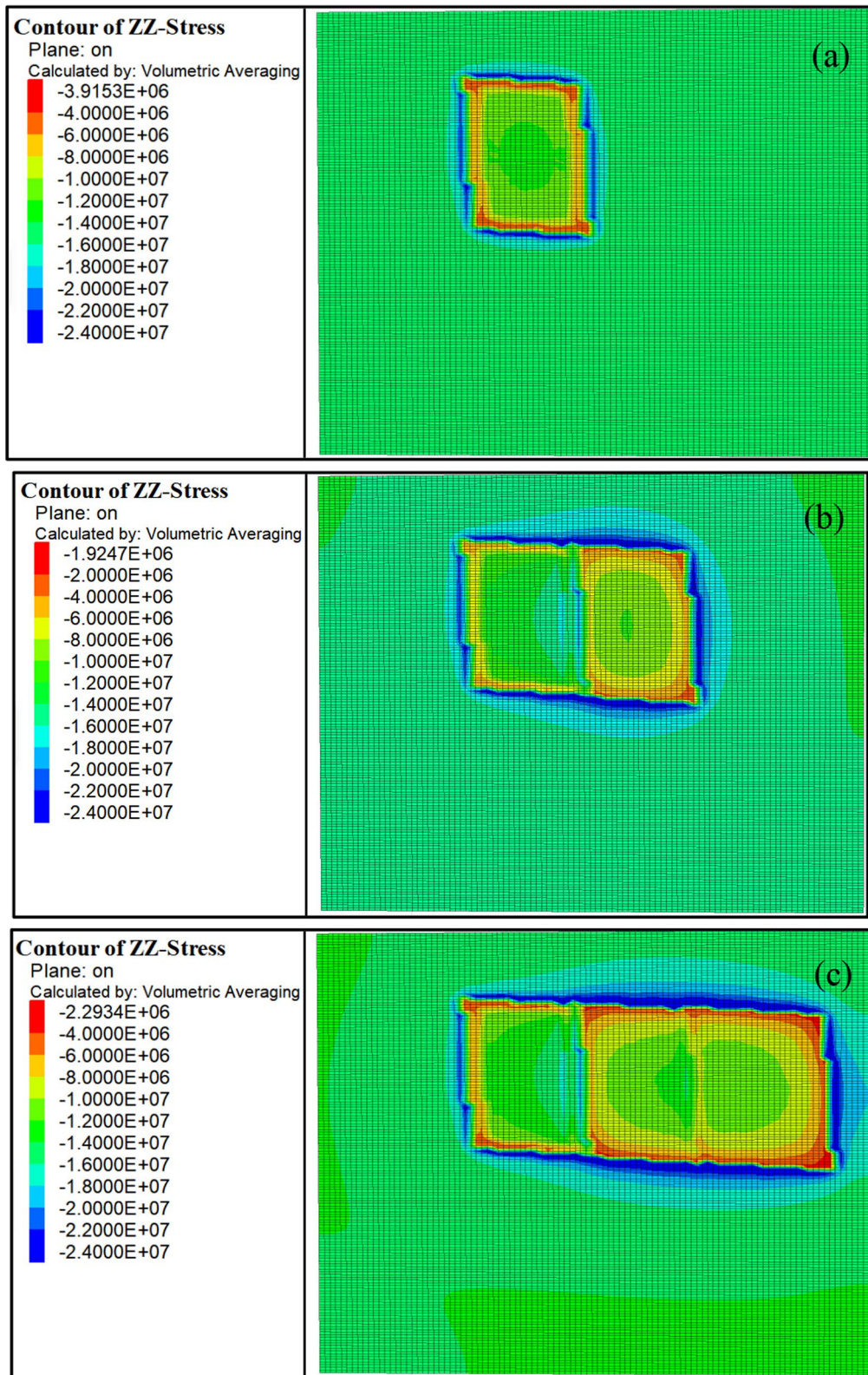


Fig. 8 Distribution of support stress in the No.1 working face. **a** working face advance to 200 m, **b** working face advance to 400 m, **c** working face advance to 640 m

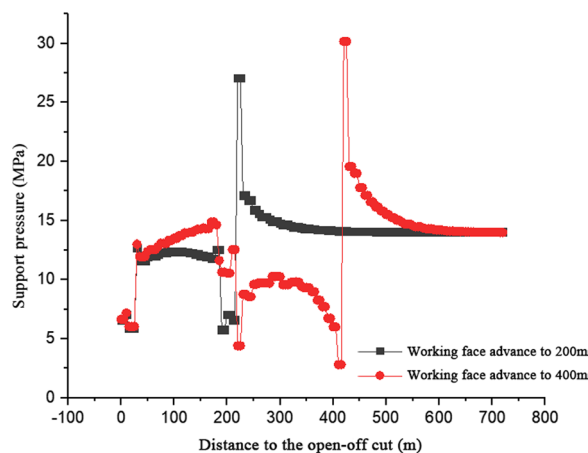


Fig. 9 Evolution of the advance support pressure of the No.1 working face when advancing 200 m and 400 m

The stress concentration was formed in the surrounding coal and rock masses of the goaf after the mining of the working face (Fig. 8). As the working face continued to advance, the concentration area of lateral and advanced support stresses in the working face continued to expand.

Figure 9 illustrated the advancement of the support pressure curve for the No.1 working face during the excavation of 200 m and 400 m. The results indicated that at a mining distance of 200 m, the maximum advance support pressure was 27.3 MPa, with a stress concentration coefficient of 1.89. The peak support pressure was observed approximately 10 m in front of the working face (Fig. 9). Upon mining for 400 m, the peak support pressure increased slightly to 29.1 MPa, with a stress concentration coefficient of 2.0. Notably, the support pressure within 100 m in front of the working face increased significantly, indicating that the dynamic pressure influence range extended up to 100 m ahead of the working face. The surrounding rock was frequently characterized by weak rheological properties due to the influence of deep dynamic pressure, which further exacerbated its deformation (Lou and Xie 2014). This effect was particularly pronounced in the presence of vertical close distance mining dynamic pressure, which could cause the stress in the surrounding rock of the tunnel to be redistributed multiple times (Lou and Xie 2014; Bu et al. 2022). The influence scope of dynamic pressure was more than 40 m (Lou and Xie 2014; Xie et al. 2018a, b). Our influence scope was slightly larger than the results of Xie et al. (2018a, b), whose influence scope was about 90 m (Xie et al. 2018a, b).

Evolution law of mining stress and range of dynamic pressure in No.2 working face

Upon completion of mining in the No.1 working face, the No.2 working face would be excavated. The distribution of support stress during the mining process in the No.2 working face was illustrated in Fig. 10. As the No.2 working face advanced, the lateral support pressure of the No.1 working face caused an asymmetric distribution of advance support pressure in the No.2 working face, with significantly higher pressure on the coal pillar side of the section (Fig. 10).

To monitor the advance support pressure on the coal pillar side of the section, a side line was established. Figure 11 displayed the evolution curve of the advance support pressure on the coal pillar side of the section as the No.2 working face advanced 200 m, 400 m, and 600 m. At 200 m, the peak advance support pressure was 31.1 MPa, with a stress concentration coefficient of 2.12 (Fig. 11). At 400 m, the peak bearing pressure was 35.8 MPa, with a stress concentration coefficient of 2.47. At 600 m, the peak bearing pressure was 37.3 MPa, with a stress concentration coefficient of 2.57. The support pressure significantly increased within 100 m of the working face, and the range of dynamic pressure influence extended 100 m ahead of the working face.

The cross-sectional view of the support pressure distribution subsequent to mining in the No.2 working face was showed in Fig. 12. The stress in the goaf of the No.2 working face exhibited a significant reduction (Fig. 12). The presence of small coal pillars between the No.1 and No.2 working faces prevented the formation of a large-scale stress concentration area in the coal and rock masses within the coal pillar region. Additionally, the lateral support stress concentration area of the No.1 and No.2 working faces had a negligible impact on the 13 coal seam. Consequently, the mining activities in the No.1 and No.2 working faces had not impact on the No.3 working face. Our results were consistent with others in pressure distribution (Xie et al. 2018a, b; Wang et al. 2021; Ti et al. 2021).

Evolution law of mining stress and range of dynamic pressure in No.3 working face

After the sequential mining of the No.1 and No.2 working faces, the No.3 working face would be mined. To investigate the evolution law of support stress during the mining process of the No.3 working face, a vertical stress distribution was sliced for the coal seam (13 coal seam) of the No.1 working face. Figure 13 illustrated the distribution of support stress during the mining process of the No.3 working face. The vertical stress in the area where

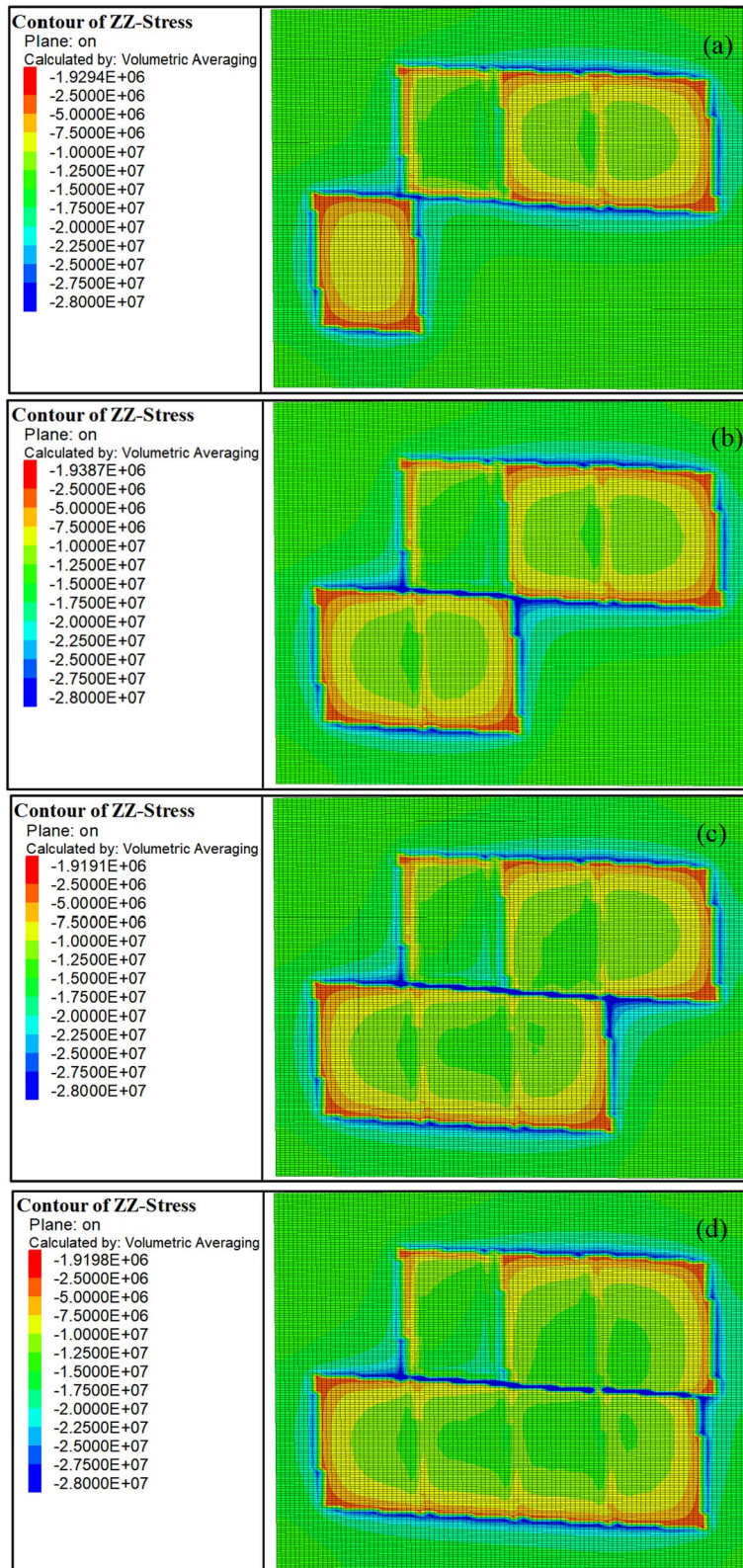


Fig. 10 Distribution of support stress during the mining process in the No.2 working face. **a** Working face advance to 200 m, **b** working face advance to 400 m, **c** working face advance to 600 m, **d** working face advance to 800 m

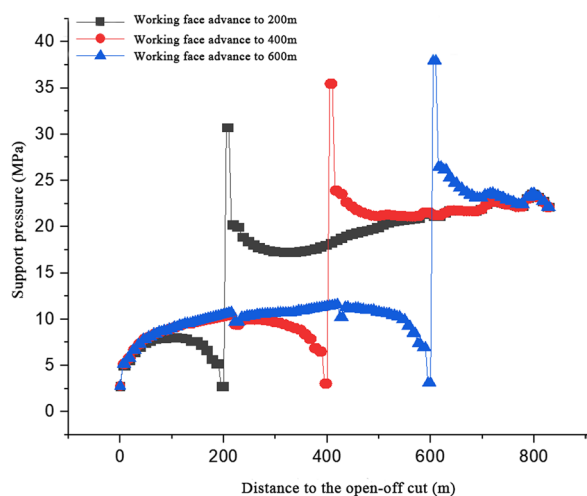


Fig. 11 Evolution of the advance support pressure of the working face on the side of the section coal pillar when the No.2 working face advances 200 m, 400 m, and 600 m

the 13 coal seam was not affected by the mining stress of the No.3 working face was approximately 12.5 MPa, which was equivalent to the initial vertical stress (Fig. 13). The impact of coal mining on the 13 coal seam was relatively small during the mining of the No.1 and No.2 working faces. Furthermore, the stress concentration degree of the advanced and lateral support pressure of the working face increased with the increasing of the mining range of the No.3 working face. And there was a significant degree of stress concentration in the expanding area of the working face.

Figure 14 illustrated the evolution of the advance support pressure for the No.3 working face during the advancement of 100 m, 200 m, 300 m, 400 m, and 500 m. At a mining distance of 100 m, the peak advance support pressure was recorded at 24.8 MPa, with a corresponding stress concentration coefficient of 1.98. At

a mining distance of 200 m, the peak support pressure increased to 25.5 MPa, with a stress concentration coefficient of 2.04 (Fig. 14). At a mining distance of 300 m, the peak support pressure further increased to 28.4 MPa, with a stress concentration coefficient of 2.27. Subsequently, the peak support pressure stabilized at around 28.4 MPa with the working face advancing. Notably, a significant increase in the support pressure was observed within a range of 120 m in front of the working face, with the dynamic pressure influence range extending 120 m ahead of the working face.

Conclusion

In this paper, FLAC^{3D} was used to build a large-scale numerical model to simulate the sequential mining process of three adjacent working faces in Liuzhuang Coal Mine located in southern China, and the stress evolution law and influence range of dynamic pressure of the working face were analyzed. Research has found that the maximum height of plastic zone development after mining in the No.1 working face was 41 m, and the maximum height of plastic zone development was 33.8 m away from the 13 coal seam. It did not affect the top and bottom of the No.3 working face. The development height of the plastic zone on the roof of the No.2 working face after mining was 52 m, and the top and bottom plates of the No.3 working face remained intact. The plastic zone of the floor of the No.3 working face after mining was not communicated with the plastic zone of the roof of the No.1 and No.2 working faces. There was a complete rock layer between the two coal seams, and there was not the mutual influence of the mining activities. During the mining process of working faces No.1 and No.2, the range of dynamic pressure influence and significant increasing in the support pressure extends up to 100 m ahead of the working face. During the mining process of the No.3 working face, there was a significant increase

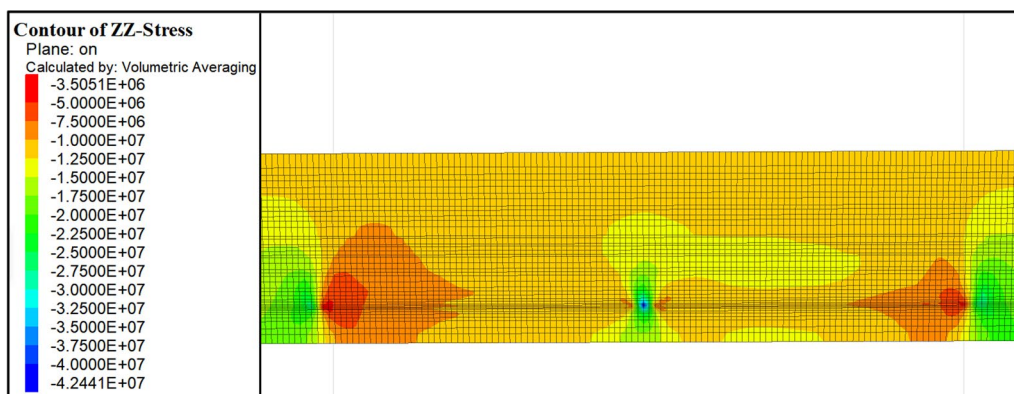


Fig. 12 Cross-sectional view of the distribution of support pressure after mining in the No.2 working face

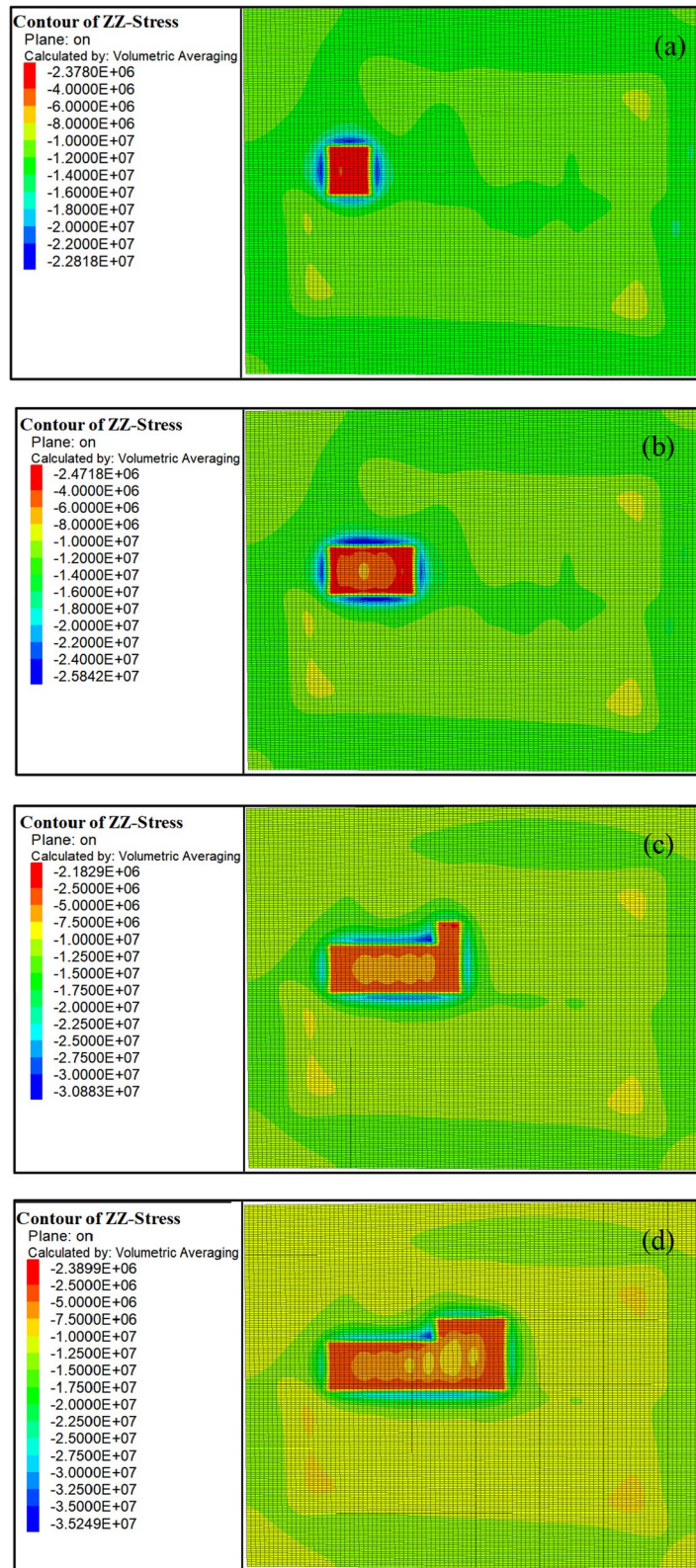


Fig. 13 Distribution of support stress during the mining process of No.3 working face. **a** Working face advance to 100 m, **b** working face advance to 200 m, **c** working face advance to 300 m, **d** working face advance to 400 m, **e** working face advance to 500 m

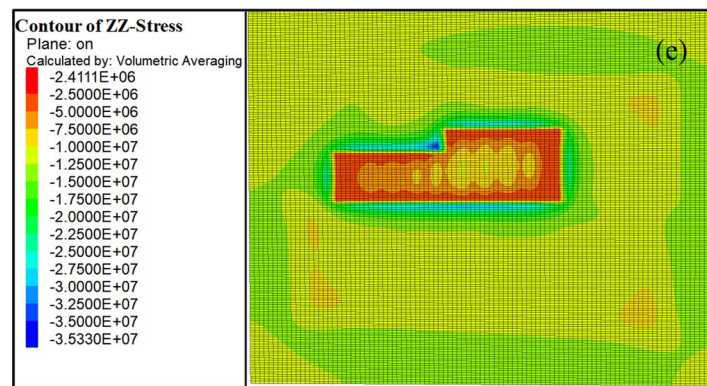


Fig. 13 continued

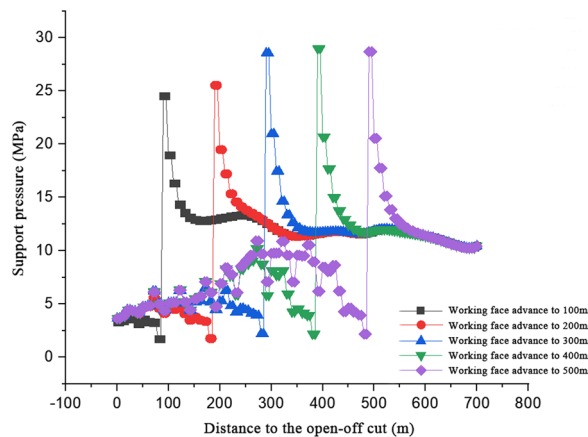


Fig. 14 Evolution curve of the advance support pressure of the No.3 working face

in the support pressure within a range of 120 m in front of the working face, and the range of dynamic pressure influence was 120 m ahead of the working face. After the mining of No.1 and No.2 working faces, the stress in the goaf significantly decreased, and the lateral support stress concentration area of No.1 and No.2 working faces had a relatively small impact on the 13 coal seam. Therefore, the No.1 goaf and mining of No.2 working faces had not disturbance to No.3 working face.

A limitation of the study was that we only conducted analysis using numerical simulation. In the future, field observations will be carried out to verify the conclusions. Our methods could be extended to similar mining coal, especially to adjacent working faces. This study provides a reference for the stress distribution and support design during the sequential mining process of adjacent working faces.

Author contributions

MZ and SM contributed to the conception, design and drafting of the work. ZT contributed to the acquisition, analysis, interpretation of data, and drafting of the work. SM contributed to the drafting of the work. LM, XL and ZS contributed to the analysis. All authors read and approved the final manuscript.

Funding

No foundation.

Availability of data and materials

All data, models, and code generated or used during the study appear in the submitted article.

Declarations

Competing interests

The authors declare that they have no competing interests.

Received: 12 May 2023 Accepted: 1 July 2023

Published online: 13 July 2023

References

Bu Q, Yuan B, Ye M, Xu N (2022) Analysis on spatial disturbance influence of surrounding rock stress in the staggered roadways and its control countermeasures. *Shock Vib* 1–12

Guo Y, Zhou H, Rong T et al (2018) Disturbance characteristics of deep coal mass under the mining stress path. *J China Coal Soc* 43(11):3072–3079

Huang Q, Cao J, Du J et al (2019) Research on three-field evolution and rational coal pillar staggered distance in shallow buried closely spaced multi-seam mining. *J China Coal Soc* 44(3):681–689

Li C, Zhang Y, Zhang G et al (2018) Crack propagation mechanisms and stress evolution of floor under dynamic disturbance in deep coal mining. *Chin J Geotech Eng* 40(11):2031–2040

Li T, Li Z, Sun J (2022) Study on dynamic evolution of overburden rock movement and mining-induced stress of ultra-high working face. *Shock Vib* 1–12

Lin J, Wang Y, Yang J et al (2015) Simulation studies on stress field evolution of roadway excavation under different confining pressures. *J China Coal Soc* 40(10):2313–2319

Liu J, Jiang F, Zhu S (2015) Study of dynamic and static abutment pressure around longwall face and its application. *Chin J Rock Mech Eng* 34(9):1815–1827

Lou PJ, Xie WB (2014) Influence factor analysis of stability of surrounding rock at crossover point for large-section roadway. *Electron J Geotech Eng* 19:1281–1293

- Luo S, Wang T, Wu Y et al (2023) Evolution characteristics of mining stress of bearing arch and interval strata in longwall mining of steeply dipping coal seam groups. *J China Coal Soc* 48(2):551–562
- Meng Q, Han L, Qiao W et al (2016) Evolution law and control technology of surrounding rock for weak and broken coal roadway with large cross section. *J China Coal Soc* 41(8):1885–1895
- Pang Y, Wang G, Li B (2023) Stress path effect and instability process analysis of overlying strata in deep stopes. *Chin J Rock Mech Eng* 48(02):551–562
- Peng R, Meng X, Zhao G et al (2016) The evolution law of deep circular roadway secondary bearing structure “time-space” integration. *J Min Saf Eng* 33(5):779–786
- Pirulli M, Barbero M, Marchelli M et al (2017) The failure of the Stava Valley tailings dams (Northern Italy): numerical analysis of the flow dynamics and rheological properties. *Geoenviron Disasters* 4(3):1–12
- Qian Z, Huang Z, Song J (2018) A case study of water inrush incident through fault zone in China and the corresponding treatment measures. *Arab J Geosci* 11(14):381–392
- Tang Y, Sun W, Zhang X, Liu P (2021) Effect of advancing direction of working face on mining stress distribution in deep coal mine. *Adv Civ Eng* 7402164
- Ti Z, Li J, Wang M, et al (2021) Fracture characteristics and zoning model of overburden during longwall mining. *Shock Vib*
- Wang L, Xie G, Wang J (2015) Numerical investigation on the influence of surrounding rock stress shell on fractured field. *J China Coal Soc* 40(9):2009–2014
- Wang F, Jie Z, Ma B, et al (2021) Influence of upper seam extraction on abutment pressure distribution during lower seam extraction in deep mining. *Adv Civ Eng*
- Wo X, Li G, Li J, Yang S, Lu Z, Hao H, Sun Y (2022) The roof safety under large mining height working face: a numerical and theoretical study. *Minerals* 12:1217
- Wu Y, Hu B, Lang D et al (2021) Risk assessment approach for rockfall hazards in steeply dipping coal seams. *Int J Rock Mech Min Sci* 138:1–17
- Xie G, Li J, Wang L et al (2018a) Mechanical characteristics and time and space evolution of stress shell in stope floor stratum. *J China Coal Soc* 43(1):52–61
- Xie J, Xu J, Feng W (2018b) Mining-induced stress distribution of the working face in a kilometer-deep coal mine—a case study in Tangshan coal mine—a case study in Tangshan coal mine. *J Geophys Eng* 15(5)
- Zhang M, Jiang F, Wang J et al (2018a) Space-time regularity of roadway deformation under disturbance of several coal seams in ultra-deep mines. *J Min Saf Eng* 35(2):229–237
- Zhang M, Liu S, Shimada H (2018b) Regional hazard prediction of rock bursts using microseismic energy attenuation tomography in deep mining. *Nat Hazards* 93(3):1359–1378
- Zhang G, Li Q, Zhang Y et al (2021) Failure characteristics of roof in working face end based on stress evolution of goaf. *Geomech Geophys Geo-Energy Geo-Resour* 7(53):1–22
- Zhou G, Li Y, Zhang Q et al (2016) Research on monitoring technique and evolution law of the disturbance stress in Chensilou Colliery. *J China Coal Soc* 41(5):1087–1092

Publisher's Note

Springer Nature remains neutral with regard to jurisdictional claims in published maps and institutional affiliations.

Submit your manuscript to a SpringerOpen[®] journal and benefit from:

- Convenient online submission
- Rigorous peer review
- Open access: articles freely available online
- High visibility within the field
- Retaining the copyright to your article

Submit your next manuscript at ► [springeropen.com](https://www.springeropen.com)
